Published online 28 December 2012 *Nucleic Acids Research, 2013, Vol. 41, No. 4* **2673–2682**
doi:10.1093/nar/gks1303

Crystal structure of an intermediate of rotating dimers within the synaptic tetramer of the G-segment invertase

Christopher J. Ritacco[1], Satwik Kamtekar[1], Jimin Wang[1] and Thomas A. Steitz[1,2,3,*]

[1]Department of Molecular Biophysics and Biochemistry, [2]Department of Chemistry and [3]Howard Hughes Medical Institute, Yale University, New Haven, CT 06520, USA

Received June 28, 2012; Accepted November 14, 2012

ABSTRACT

The serine family of site-specific DNA recombination enzymes accomplishes strand cleavage, exchange and religation using a synaptic protein tetramer. A double-strand break intermediate in which each protein subunit is covalently linked to the target DNA substrate ensures that the recombination event will not damage the DNA. The previous structure of a tetrameric synaptic complex of $\gamma\delta$ resolvase linked to two cleaved DNA strands had suggested a rotational mechanism of recombination in which one dimer rotates 180° about the flat exchange interface for strand exchange. Here, we report the crystal structure of a synaptic tetramer of an unliganded activated mutant (M114V) of the G-segment invertase (Gin) in which one dimer half is rotated by 26° or 154° relative to the other dimer when compared with the dimers in the synaptic complex of $\gamma\delta$ resolvase. Modeling shows that this rotational orientation of Gin is not compatible with its being able to bind uncleaved DNA, implying that this structure represents an intermediate in the process of strand exchange. Thus, our structure provides direct evidence for the proposed rotational mechanism of site-specific recombination.

INTRODUCTION

Site-specific recombination is performed by either one of the two families of site-specific recombinases, each of which uses either a tyrosine or serine that forms a phosphodiester intermediate (1). The recombinases share the events of recombination: synapsis, strand cleavage, strand exchange and religation. The tyrosine recombinases use a stepwise mechanism in which cleavage, exchange and religation of a single strand create a Holliday junction, followed by a second set of cleavage, exchange and religation reactions that resolves this Holliday junction (1). The crystal structures of the Cre recombinase reveal that the two duplex DNAs are bound between the subunits of a tetrameric protein scaffold and are separated by only a few Angstroms (2–6). The essential movements of DNA and protein for recombination are limited to the interior of the complex. In contrast, the serine recombinases make double-strand breaks on both DNA duplexes and exchange both strands in concert (Figure 1) (7). The tetrameric protein lies between the two DNA duplexes that will be recombined; this creates a separation of >40 Å between the partners that will be exchanged and religated (8). A rotational hypothesis of strand exchange involving a rotation of 180° was formulated but with no specific architectural insights (9–11). The details came from the crystal structure of the synaptic complex of γδ resolvase covalently linked to a DNA substrate (8). This structure revealed a flat hydrophobic interface that lies between two dimers and is oriented perpendicular to the helical axes of the two DNA duplexes. Li *et al.* proposed this interface as the exchange interface in which the dimer on one side of the interface rotates 180° relative to the other dimer which realigns the two cleaved DNA duplexes for religation.

Although this model of rotation is consistent with all biochemical and structural data available, the structure of an intermediate along the rotational pathway has been lacking. In the subunit rotation model, the interactions at the exchange interface are identical before and after the proposed rotation, implying that there is no free energy difference between the two states. The net driving force for this rotation is likely derived from relaxing the supercoiled DNA substrate (12,13). Moreover, the hydrophobic side chains forming the exchange interface provide little energetic barrier for rotation, creating a challenge for

*To whom correspondence should be addressed. Tel: +203 432 5617; Fax: +203 432 3282; Email: thomas.steitz@yale.edu
Present address:
Satwik Kamtekar, Pacific Biosciences of California, 1380 Willow Road, Menlo Park, CA 94025, USA.

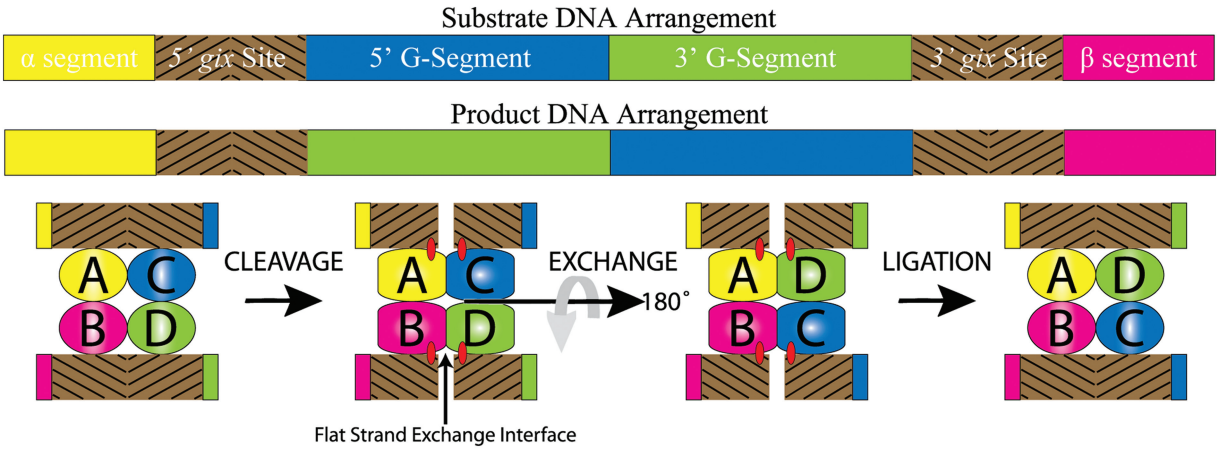

Figure 1. The mechanism of Gin inversion. Top: bar scheme depicting the arrangement of the phage Mu DNA prior to and after a successful inversion event. Bottom: a dimer of Gin binds to each *gix* site (data not shown) and forms a homo-dimeric tetramer at synapsis. The activating factor Fis (data not shown) causes a conformational change in Gin allowing catalysis. The cleavage reactions result in a double-strand break covalently linked to the protein through a phosphodiester bond at the *gix* site. The strands are exchanged through 180° of rotation of the DNA about the exchange interface and then are religated to complete the inversion.

the isolation of a rotational intermediate (8,14). We targeted a rotational intermediate using the G-segment invertase (Gin) which is closely related to γδ resolvase (7).

Prior to the determination of the structure of the synaptic γδ resolvase, extensive structural studies had identified three structural domains, the N-terminal catalytic domain (NTD) (M1–S101), the E helix (Y102–G137) and the DNA-binding domain (DBD) (V138–N183) (15–18). The E helix was initially classified as part of the NTD along with the A, B, C and D helices, but was re-classified as a separate domain because it rotates and twists independently relative to the NTD (8). The initial structures of the NTD and E helix of γδ resolvase revealed the enzyme's inherent conformational flexibility (16–18). Flexibility was also observed in the structure of an asymmetric dimer of resolvase in complex with DNA (15). In this structure, the E helix and DBD bind the DNA duplex and the attacking serine residues lie 13 Å from the scissile phosphates. Major rearrangements will be required to bring the active site serines of the enzyme close to the scissile phosphates. The conformational flexibility was also evident in the structure of a resolvase-Hin chimera in a complex with DNA as well as in a truncation of the synaptic tetramer of resolvase (19). Thus, conformational flexibility is an intrinsic property that is essential for recombination in this family of enzymes.

While this article was in preparation, the structure of a truncated mutant of the tetrameric Sin resolvase in the absence of a DNA substrate was published and provides a high-resolution view of the catalytic site that appears appropriately positioned for DNA cleavage and/or religation (20). The rotational state of this tetramer at the exchange interface differs from the synaptic complex of γδ resolvase and could be supporting evidence for the proposed model of subunit rotation. The structure of Gin reported here with a flat exchange interface like that of γδ resolvase provides additional support for rotation about the exchange interface as the mechanism of subunit rotation.

The data from structure-based mutational studies also support the rotational mechanism (13,21). Although the exchange interface is made exclusively of the four E helices, the synaptic interface, which holds the rotating dimer subunits together, is formed by both hydrophobic and hydrophilic residues from the D and E helices, including salt bridges (8). When cysteine mutations were introduced into the D helices at positions that allow the formation of disulfide bonds across the synaptic interface, there was no effect on the strand exchange reaction (21). However, when cysteine mutations were engineered in the E helix to allow crosslink formation across the exchange interface, strand exchange was inhibited but not strand cleavage. Further biochemical support came from the Hin-Fis system where the positive or negative linking number of the supercoiled DNA directly determines the direction of rotation of the synaptic complex. Finally, single-molecule data on the Bxb1 integrase suggest a 'molecular bearing' surface for strand exchange (22). These data also show that the system can rotate multiple times without religating, implying that the two events are not correlated.

Gin is a member of the serine family of site-specific DNA recombinases with 37% sequence identity and 57% sequence similarity to γδ resolvase (7,23,24). Gin inverts the 3-kb G-segment of the chromosomal DNA of the phage Mu (24). This inversion directly influences the structure of two-tail fiber proteins of the phage for selective bacterial infection (Figure 1) (25–27). Like γδ resolvase, Gin forms covalent intermediate complexes with the target phosphates of its DNA substrate and becomes catalytically inactive if the hydroxyl of the linking serine (S9) is removed or altered (28,29).

In order to obtain the structure of a synaptic tetramer of Gin, we used a mutant Gin protein, M114V, which does not require the host factor Fis protein for activation or synaptic tetramer formation (30,31). The additional substitution of S9A was included to prevent DNA cleavage but not DNA binding or synapsis. These mutations allow

the capture of a synapsed tetramer of Gin with an uncleaved DNA substrate. We have crystallized the tetrameric synaptic complex of Gin in the absence of a DNA substrate. The orientation of the rotating dimers in the complex of a full-length Gin with the S9A/M114V mutations differs by 26° relative to the orientation of the rotating dimers of the synaptic structure of γδ resolvase and provides structural evidence for the subunit rotation mechanism of strand exchange.

MATERIALS AND METHODS

Protein expression and purification through denaturation and protein refolding procedures

A M114V/S9A double mutant of Gin was constructed in an expression plasmid under the promoter for phage T7 RNA polymerase. This plasmid was transformed into the *Escherichia coli* expression line BL21 (DE3) Star (Invitrogen). Transformed cells were grown in a 10-l fermentor in the presence of 0.3 μg/ml kanamycin to an OD_{600} of 1.0 and induced with 1 mM isopropyl-β-D-thiogalactopyranoside (Sigma) for 3 h. The cells were harvested by centrifugation and then flash frozen.

For purification of Gin protein, 40 g of the frozen cell paste was thawed in resuspension buffer (1 M NaCl, 40 mM Tris–Cl, pH 7.5, 0.05% β-octyl glycoside (βOG), 2 mM EDTA, 2 mM DTT) to a final volume of 120 ml. The resuspended cells were divided into two 60-ml fractions and lysed using an incubation with 10 mg of lysozyme and 0.1% PMSF for 30 min at room temperature, followed by sonication with three passes of 60 s at 50% duty cycle with the maximal power setting. The insoluble fraction was pelleted by centrifugation at 19 000 rpm in an SS-34 rotor for 30 min at 4°C. The resulting supernatant was collected and dialyzed twice, in each instance for 2 h, against 2 l of a no-salt buffer (40 mM Tris–Cl pH 7.5, 0.05% βOG, 2 mM EDTA, 2 mM DTT) using the Spectrapore 10 kDa (Spectrum Labs) cutoff membranes, resulting in full precipitation of Gin protein. The precipitated protein was pelleted by centrifugation at 12 000 rpm in a GSA rotor for 15 min at 4°C. The pellet was resuspended in 40 ml of denaturing CM-Buffer A (6 M urea, 40 mM Tris, pH 7.5, 2 mM DTT). The protein resuspension was loaded onto a CM-Sepharose (GE Healthcare) column that was pre-equilibrated with CM-Buffer A. The protein was then eluted off the column with a linear gradient of 0–100% CM-Buffer B (6 M urea, 1 M NaCl, 2 mM DTT, 40 mM Tris, pH 7.5) over 200 ml. The protein fractions were collected and diluted to an A_{280} measurement <0.1 with CM-Buffer B. The diluted sample was dialyzed using Spectrapore membranes with a 10-kDa cutoff against 2 l of refolding buffer (1 M NaCl, 20 mM Tris, pH 7.5, 2 mM DTT, 0.05% βOG) for slow refolding of the protein. The refolded protein was precipitated by using 35% (0.197 g/ml) $(NH_4)_2SO_4$ and collected by centrifugation at 12 000 rpm in a GSA rotor for 15 min at 4°C. The protein pellet was resuspended and concentrated in storage buffer [10% $(NH_4)_2SO_4$, 20 mM Tris, pH 7.5, 2 mM DTT, 0.01% βOG] to a maximal concentration of ~2 mg/ml. The sample was divided into 150 μl aliquots and flash frozen for storage at −80°C.

Crystallization and data collection

The solution of Gin protein was thawed at room temperature and diluted with ethylene glycol (EG) to a final concentration of EG of 25% and ~1 mg/ml of Gin protein. Hexagonal crystals were grown by mixing the protein solution with an equal volume of the equilibrating well solution containing 5–10% $(NH_4)_2SO_4$, 100 mM MES, pH 6.5, 10 mM $MgSO_4$, 10–25% EG.

The resulting crystals were stabilized with the stabilization buffer containing 3% $(NH_4)_2SO_4$, 100 mM MES, pH 6.5, 35% EG, 10 mM $MgSO_4$ and then frozen in liquid propane. The di-μ-iodobis(ethylenediamine)diplatinum (II) nitrate (PIP) and other platinum derivatives were prepared by soaking stabilized crystals in a new stabilization buffer containing 1 mM heavy atom compounds or 100 μM for ethyl-mercury phosphate for up to 1 h. Crystals that were treated with Pt or Hg were then back-soaked into the original stabilization buffer prior to being frozen in liquid propane.

Native X-ray diffraction data were collected at the Advanced Photon Source (APS) station 24-ID. Crystals belong to the space group $P6_222$ with cell dimensions $a = b = 116.8$ Å, $c = 117.6$ Å, $\alpha = \beta = 90°$, $\gamma = 120°$. Data processing was performed with both the HKL2000 and XDS suites (32,33), as summarized in Table 1. XDS processing provided better statistics and higher resolution than HKL2000. The effective resolution of the data is 3.7 Å using a stringent cutoff criterion of $<I/\sigma I> = 2.0$ in the highest resolution shell (Table 1). We have extended the resolution during refinement to include data to 3.5 Å using a less stringent cutoff criterion of $<I/\sigma I> = 0.89$ as has been suggested (34,35) (Table 1). This change in cutoff also yields slight changes to the $2F_o–F_c$ maps and were included in the refinement of the structure (Supplementary Figure S1). Heavy atom derivative diffraction data were collected at the Advanced Light Source station 8.2.1/8.2.2 and the Advanced Photon APS station 19 – ID and processed in the same way as the native data (Table 1).

Generation of Gin homology model

The amino acid sequence of Gin, accession number AAF01129, was provided to the EXPASY server and the SWISS-MODEL (36) tool for construction of homology models of Gin using the synaptic structure of γδ resolvase (1ZR4) (8) or that of the Site I Dimer (1GDT) (15) as the template. A single run of homology modeling was performed starting with the chain A of the 1ZR4 structure.

Structure determination and refinement

The heavy atom positions were located using the single-isomorphous replacement with anomalous scattering method for each derivative using the automated program SOLVE (37), and experimental phases were improved by cycles of the solvent flattening of the

Table 1. Data processing, phasing and refinement statistics

Data processing						
Native					*PIP*[a]	
Resolution(Å)	R^{b}_{merge} (%)	I/σI	Comp. (%)	Redund.	Resolution (Å)	46.0–4.1
12.00	8.3	19.02	71.1	4.3	R_{merge}(%)[b]	6.3
10.00	7.8	20.53	93.7	5.1	I/σI	15
8.00	7.6	20.71	95.0	5.3	Completeness (%)	92
7.00	7.9	19.60	97.0	5.5	Redundancy	3.2
6.00	8.0	16.95	98.7	5.6	R_{iso} (%) (to *Native*)[h]	33.3
5.00	10.2	13.06	99.6	5.7		
4.50	13.5	10.48	99.6	5.8		
4.00	37.1	4.99	99.6	5.8		
3.70	103.8	2.00	99.7	5.9		
3.50	228.6	0.89	99.9	6.0		
Total	11.0	8.56	98.3	5.7		
Phasing						
Resolution (Å)			38.8–4.1			
'SOLVE' *Z*-Score[c]			19.14			
'SOLVE' Figure of Merit[c]			0.54			
Refinement						
Resolution			3.5 Å – 101 Å			
No. of Reflections			5824			
No. of Atoms			984			
R_{work} (%)[d]			25.6 (39.5)			
R_{free} (%)[e]			28.9 (45.8)			
R^{f}_{o2p}			1.48			
RMSD bond length (Å)[g]			0.006			
RMSD bond angle (°)[g]			1.0			
PDB accession number			3UJ3			
Ramachandran						
Most favored and allowed (%)			98.2			
Additionally disallowed allowed (%)			1.8			

[a]Crystal soaked in di-μ-iodobis(ethylenediamine)diplatinum(II) nitrate.
[b]$R_{merge} = <\Sigma_{hkl}\Sigma_j|I_j(hkl)- <I(hkl)|>/<I(hkl)>$, merging statistics for all symmetry mates.
[c]Values presented as given and defined by SOLVE.
[d]$R_{work} = \Sigma_{hkl}|F_{obs}(hkl)-F_{calc}(hkl)|/\Sigma_{hkl}|F_{obs}(hkl)$, Crystallographic *R*-factor. Values in parentheses are for the highest resolution bin.
[e]R_{free} is the cross-validation *R*-factor for ~5% of randomly selected data not used in structure refinement. Values in parentheses are for the highest resolution bin.
[f]Observation to parameter ratio is defined by the ration between the unique number of observations for refinement and the number of variables, which is four times of the number of atoms.
[g]RMSD: root mean square deviation from ideal values
[h]R_{iso} is the R_{merge} value between the native and derivative data set.

electron density maps using automated procedures of RESOLVE (38). All heavy atom compounds bound the same Cys-24 site so that it was not possible to further improve experimental phases using the multiple-isomorphous replacement with anomalous scattering methods. The homology model of Gin was fit as a rigid body into the solvent-flattened electron density map using the automated search for model in map option of MOLREP (39); initial rigid body refinement in REFMAC (40) of the placed model had an *R*-value of 51% and an R_{free} value of 49%. The 3D graphics software COOT (41) was used for a fine tuning of the fitting of the structure into the electron density. Several rounds of rigid body refinement of the fit model were carried out in REFMAC with the last round including restrained positional refinement. The final refined model includes a monomer in the asymmetric unit and yields a working *R*-factor of 25.6% and free *R*-factor of 28.9% using the complete range of collected data to better than 3.7 Å of resolution. Refinement statistics are summarized in Table 1. All figures were generated in RIBBONS (42) or PYMOL (43).

222-dyads-based alignment and movies interpolation

To align the local dyad of dimeric AB subunits to a given specific axis such as the *x*-axis, a rotated A′ and B′ were generated from A and B using the 2-fold crystallographic symmetry about the *x*-axis. Least squares superposition of the dimer-AB onto the subunit A′ and B′ results in the perfect alignment of dimeric local dyad along the *x*-axis. Similarly, to align the local 222-dyads of tetrameric ABCD subunits onto the specific axes such as Cartesian *xyz*-axes, the rotated A′, B′, C′ and D′ were generated using the corresponding 2-fold crystallographic symmetry around the *x*, *y* and *z*-axis. A simultaneous least-squares superposition of the tetramer-ABCD onto the subunits A′B′C′D′ results in a perfect alignment of local 222-dyads to the *xyz*-dyads. This alignment

procedure alleviates the differences in the proteins and strictly aligns the tetramers on their symmetry.

After aligning the local dyad of tetrameric γδ resolvase synaptic complex that defined the normal of the flat synaptic surface on the *z*-axis, a linear interpolation algorithm was used to generate a series of γδ resolvase coordinates to rotate along the *z*-axis to describe the results reported here (see Supplementary Movies).

RESULTS AND DISCUSSION

Overall structure of the synaptic tetramer of Gin

The synaptic tetramer of Gin lies on the 222-point symmetry in the $P6_222$ space group with one monomer per asymmetric unit (Figure 2A). The initial electron density map was determined using the SAD method with the PIP derivative. The experimental phases generated from SAD were used as refinement restraints and were of sufficiently high quality that the experimental maps differed very little from the final $2F_o–F_c$ maps that were calculated using phases derived from the refined atomic model (Figure 2A and Supplementary Movie S1). Additional features of the E helix and the location of the DNA binding domain are visible in the $2F_o–F_c$ maps at very low contour levels (0.3–0.5σ). As the inclusion of these features in the model did not benefit the refinement of the structure, they were not included in the final model.

The final model of a Gin subunit included residues L2–A125; 98.2% of the polypeptide backbones of these residues lie within the most favorable and allowed regions of the Ramachandran plot (Table 1). The root mean square deviations (RMSDs) from ideal bond lengths and bond angles are 0.006 Å and 1.0°, respectively (Table 1). The refined model has an overall temperature B-factor of 146 $Å^2$ for all atoms and 142 $Å^2$ for the main chain atoms.

The structure of the synaptic complex of Gin shows that the dimer and tetramer interfaces are formed by interactions of the E helices from each of the four subunits of Gin at the core of the structure, consistent with the previous synaptic structures of serine recombinases (8,19,20). There are two distinct interfaces between subunits in the synaptic complex of Gin. The major interface is the rotating interface between the rotating dimers of subunits AB and CD and the other is the synaptic interface which separates each rotating dimer pair between subunits A and B and subunits C and D (Figure 2B and C). The synaptic interface is formed by antiparallel interactions between the E and D helices of

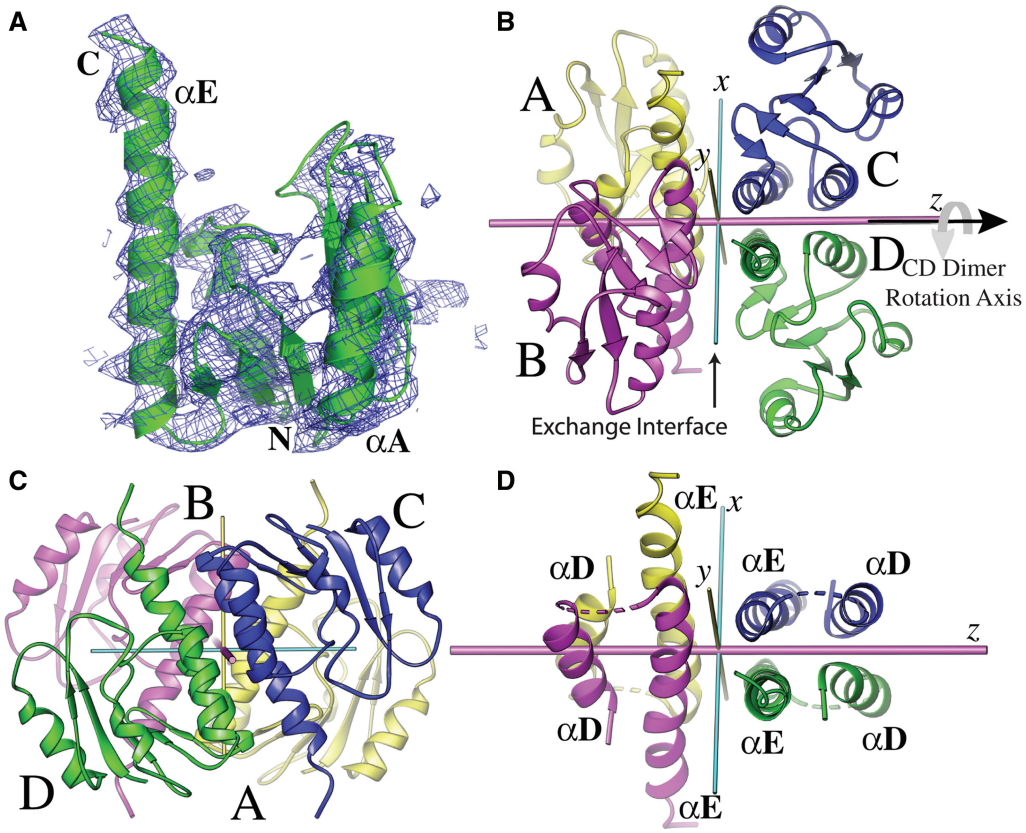

Figure 2. The structure of the synaptic tetramer of Gin. (**A**) The final $2F_o–F_c$ electron density map, calculated at 4.0 Å and contoured at 1σ, is superimposed onto the subunit structure of Gin within one asymmetric unit. (**B** and **C**) Two orthogonal views of the tetrameric synaptic complex of Gin are displayed to illustrate the difference in interfaces in the synaptic tetramer. The subunit dimer-AB and the subunit dimer-CD create the flat exchange interface of Gin. (**D**) The exchange interface (the x and y plane) is exclusively created by the E helices. The synaptic interface between subunits A/B or subunits C/D is created by both the E and D helices. The three orthogonal 222-axes (arbitrarily designated here as *x*,*y*,*z*), N and C termini, some helices and subunits A (yellow), B (magenta), C (blue) and D (green) are labeled.

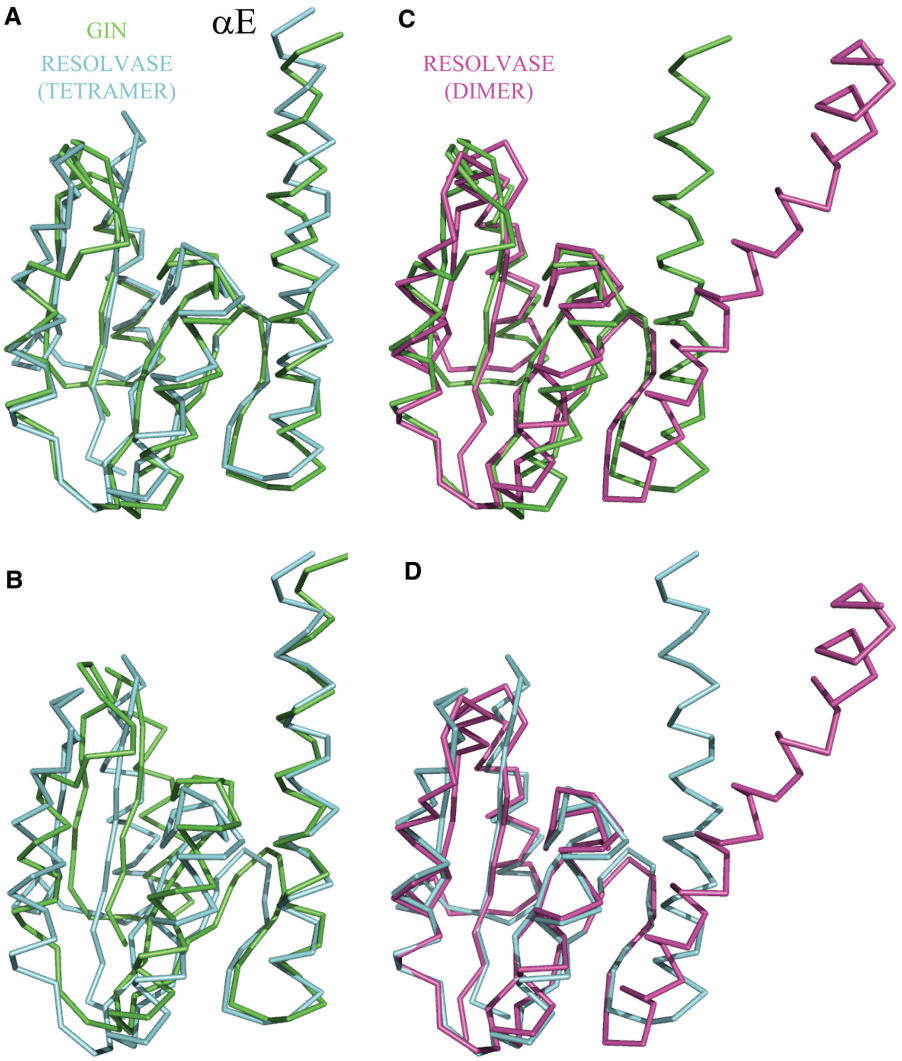

Figure 3. The conformation of the subunit of Gin. (**A**) Superposition of the NTD of Gin (green) onto the NTD of a subunit of the synaptic structure of γδ resolvase (cyan). (**B**) Superposition of the E helices of Gin and the synaptic γδ resolvase. (**C**) Superposition of the NTD of Gin onto a subunit of the Site I dimer of γδ resolvase (magenta). (**D**) Superposition of the NTDs of a subunit from the dimer and tetramer structures of γδ resolvase.

one subunit with the corresponding helices in the other subunit (Figure 2B and C). The rotational interface is flat and is formed by the hydrophobic side chains from the four E helices (Figure 2D) (8). This interface buries 1897 Å^2 per tetramer, which is similar to that of the synaptic tetramer of resolvase 1982 Å^2 (8). If DNA duplexes were present in this structure, the rotation axis (arbitrarily named the *z*-axis) would be approximately parallel to the helical axes of the DNA (Figure 2B and C). The rotational orientation of the rotating dimers across the flat rotational (exchange) interface in the synaptic complex of Gin would only allow a cleaved duplex to be bound.

Gin subunit structure

Like resolvase, the Gin subunit consists of three domains—a catalytic core NTD (residues 1–100), an E helix (residues 101–137) and a DBD (residues 138–198). The E helix is visible in this structure only to residue 125 (Figure 3A). The remaining resides of the E helix and the DBD are disordered, as in other structures of *apo* serine recombinases (16,18). Using a Cα alignment algorithm (44), we found that the RMSD between the Cα coordinates of 81 equivalent residues of the NTD of Gin and that of γδ resolvase is 1.8 Å and it is 1.2 Å for the 28 equivalent residues of their E helices. A comparison of the two independent alignments of these two domains reveals that the E helices of the two recombinases exhibit a 15° different rotational orientation about the α-helical axes relative to their NTDs (Figure 3A and B).

The mutant Gin used in this study has two amino acid substitutions, S9A and M114V. The S9A substitution in the NTD disables the cleavage of the DNA but has no effect on oligomerization (28). The M114V substitution in the E helix permits formation of a synaptic tetramer without requiring Fis for activation (31). The M114V substitution in the subunit structure of Gin does not appear to alter the secondary structure of the E helix.

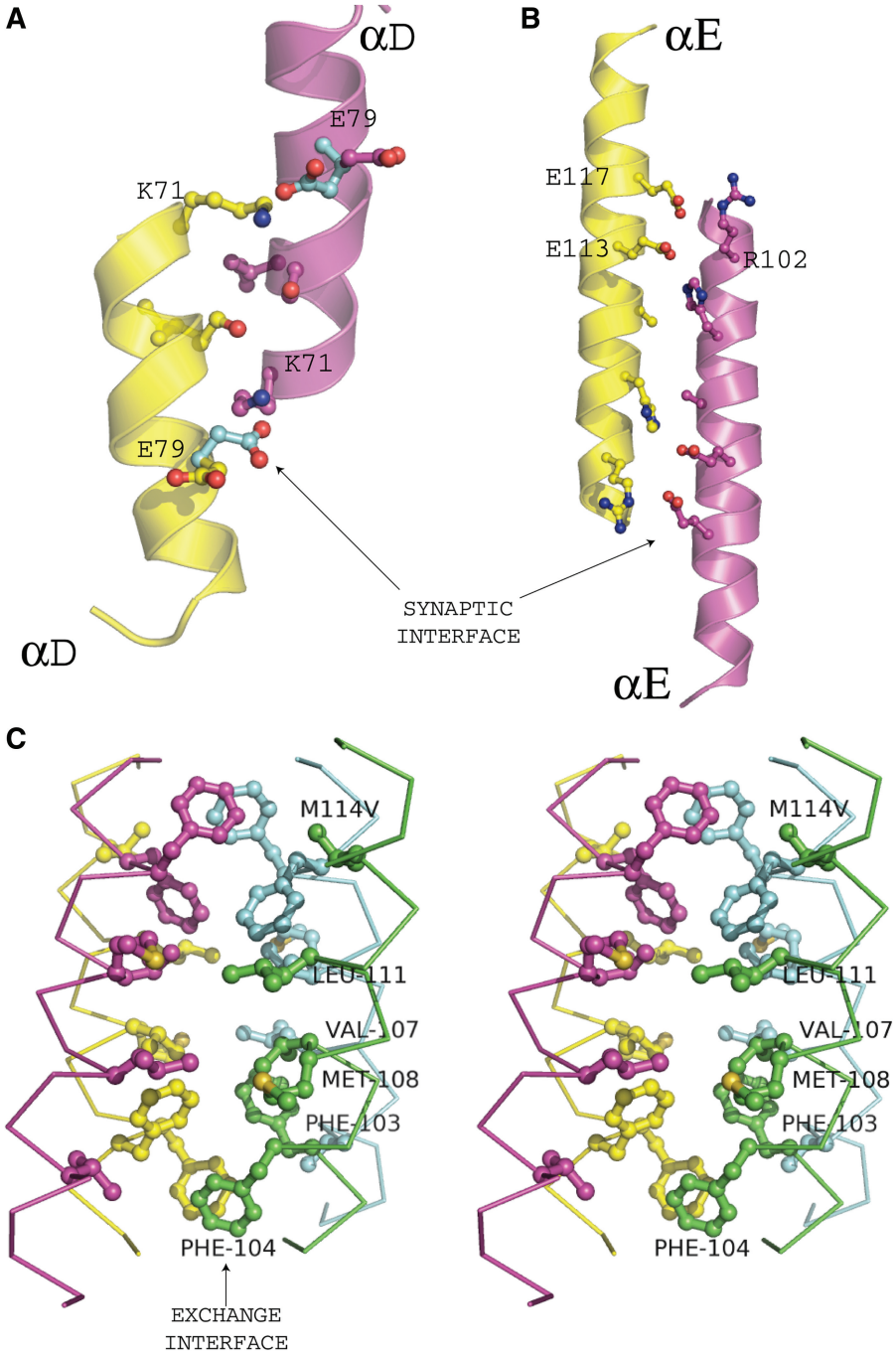

Figure 4. The synaptic and exchange interfaces of the synaptic complex of Gin. (**A** and **B**) The putative contacts made between the D (A) and E (B) helices at the synaptic interface. At the interface between the D helices, a simple modeling of an alternate rotamer of E79 (cyan A) creates a salt bridge between E79 and K71. (B) The modeled residues at the synaptic interface between the E helices may interact through electrostatic, hydrogen bonds and salt bridges between E117 and R102. (**C**) Stereo view of the exchange interface of Gin highlighting the hydrophobic residues at its core.

The orientation of the E helix relative to the NTD differs significantly between the synaptic structure of Gin and the dimeric structure of γδ resolvase (Figure 3C) (15). This change in conformation of the E helix relative to the NTD has been previously observed in other structures of serine recombinases (8,19,20,45) and has been shown biochemically to be linked to the formation of synaptic tetramers (Figure 3D) (46). The orientation of the E helix and an inability to model an uncleaved duplex DNA (Supplementary Figure S2) suggest this structure of Gin is in a post-cleavage synaptic conformation and this Gin structure is a rotational intermediate in the process of strand exchange.

Structural basis of rotation at the exchange interface

The exchange interface between the Gin dimers consists of exclusively hydrophobic residues (Figure 4C). The precise

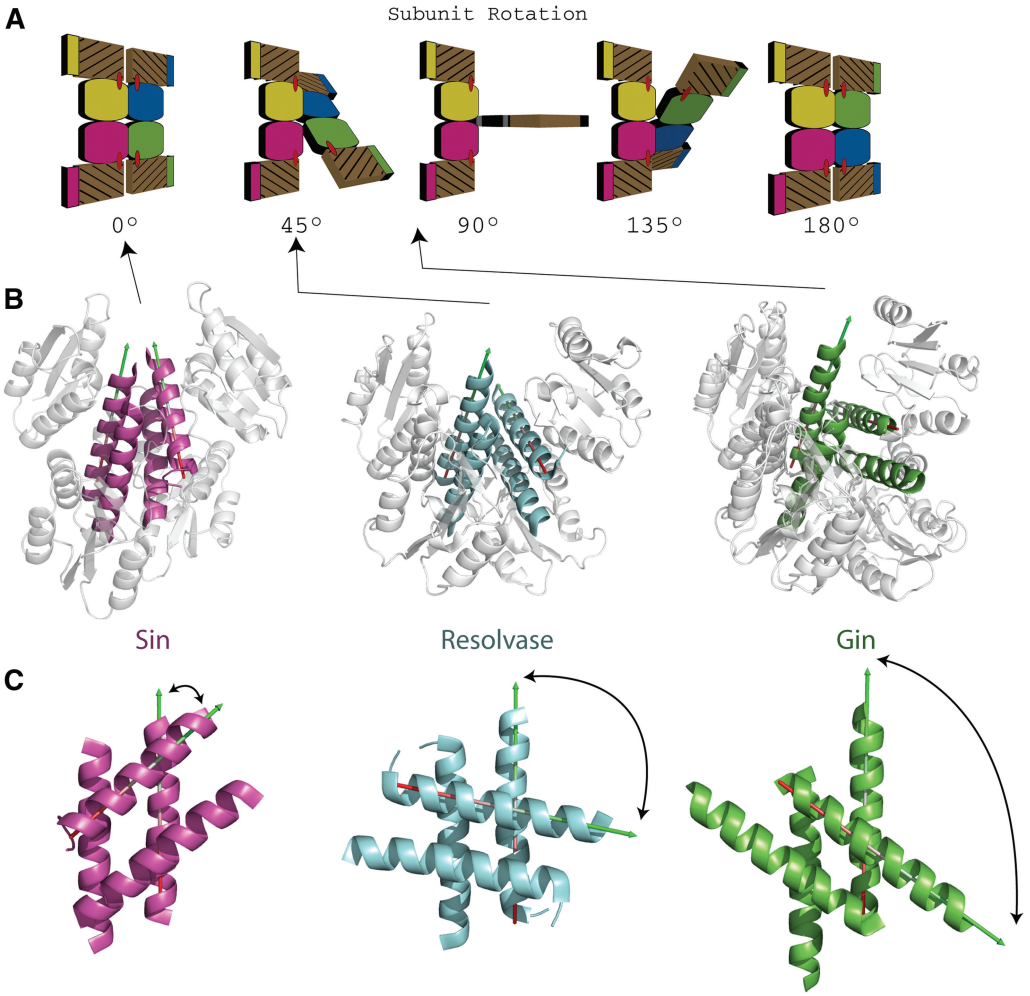

Figure 5. The subunit rotation model at the exchange interface of the serine recombinases. (**A**) Cartoon illustration of the rotation of subunits around the exchange interface. (**B**) Three synaptic tetramers with emphasis on the orientation of their E Helices [Sin (magenta), Resolvase (cyan) and Gin (green)]. The appropriate position of each tetramer on the pathway of subunit rotation is shown. (**C**) The cross angles of the E Helices of the three synaptic tetramers shown perpendicular to (B). The arrows indicate the direction (N to C) of the sequence in each E Helix.

packing of the side chain moieties cannot be determined in this structure due to the limited resolution. However, based on the extensive sequence and structural similarity between Gin and γδ resolvase, the Cα locations of the E helix at the synaptic interface and the NTD are unambiguous. As is the case with resolvase, the exchange interface is flat and is formed predominantly by the large hydrophobic residues, F103, F104, M106 and V107, L111 and L118 (Figure 4C). Consistent with the rotational model for recombination, this flat hydrophobic interface would allow the rotation of the AB dimer relative to the CD dimer (Figures 2 and 4; Supplementary Movie S2).

Only rotation of the rotating dimers about the dyad axis relating them that is perpendicular to the flat interface would enable strand exchange (Figure 1). This implies that the synaptic interface remains intact during subunit rotation and that the two DNA duplexes maintain a local 2-fold symmetry around the rotation dyad (thick magenta dyad in Figure 2). The synaptic interface is held static by polar interactions at the termini of the E and D helices (Figure 4A and B; Supplementary Movie S1). A similar pattern of interactions is seen in the synaptic interface of the synaptic structure of γδ resolvase (8).

Evidence for the rotation mechanism within synaptic complexes

An alignment of the synaptic tetramer of Gin on that of γδ resolvase using their 222-dyads clearly shows that the pairs of E helices of each synaptic tetramer have different cross angles across the rotational interface (Supplementary Figure S3). The cross angle of the E helices of Gin differs by a 13° increase in their relative orientation as compared with the rotating dimers of γδ resolvase. Although the residues that form salt bridges across the rotational interface of γδ resolvase are not conserved in Gin (7,8), it is unclear whether a salt bridge (or a lack thereof) is responsible for the rotational orientation seen in the synaptic tetramer of Gin or whether alternate rotational orientations captured at the exchange interface are more influenced by crystal packing.

The superposition of the two AB pairs of rotating dimers shows that these two subunits maintain a nearly identical relative orientation (Supplementary Figure S4A). However, when the AB pairs of dimers of the two synaptic tetramers are superimposed, their CD dimers are not aligned (Supplementary Figure S4B). A rotation of 26° of the CD dimer of resolvase relative to the superimposed AB dimer about the exchange interface (*z*-axis) aligns the two CD synaptic dimers on each other (Supplementary Movies S2 and S4). This rigid body modeling provides evidence for the flat interface being the point of rotation within the synaptic complexes.

A comparison of the cross angles between the E helices at the exchange interface exhibited by the synaptic tetramers of Gin, resolvase and Sin also supports this rotational mechanism. The E helix cross angle between the rotating dimer pair of Sin at the rotational interface is 48° less than that of the resolvase tetramer and 74° less than that of the Gin tetramer. (Figure 5B and C; Supplementary Figure S5). The cross angle formed by the resolvase E helices is midway between those of Sin and Gin. Rice *et al.* (20) concluded that the synaptic complex of Sin has its active site properly aligned for catalysis and represents a tetramer that would be a cleavage competent state if the DNA duplex were bound. They suggested that the post-cleavage synaptic tetramer of γδ resolvase has begun rotation for strand exchange. In the synaptic complex of Gin presented here, the rotating dimers have reached a further rotational orientation when compared with that of the Sin or γδ resolvase synaptic tetramers. Assuming a right-handed rotation, the rotating dimers of Gin have completed more than one-third of the 180° rotation required for strand exchange (Figure 5C).

The structural evidence that we present here supporting the mechanism of subunit rotation is derived from a comparison of three synaptic structures of serine recombinases Gin, γδ resolvase and Sin. Each synaptic tetramer forms a flat interface about which the dimers can rotate during strand exchange. The rotational orientation of γδ resolvase at the exchange interface that was captured represents a state of the strand exchange pathway that is between the Sin and Gin rotational orientations. However, we were unable to model a rigid body rotation of the rotating synaptic dimers of Sin by 48° without steric clashes. It should be noted, however, that the Sin exchange interface appears highly pliable and may be able to adapt a number of alternate conformations (Supplementary Figure S6). Additionally, the rigid body rotation of Sin does not result in a perfect alignment with γδ resolvase or Gin (Supplementary Movie S4) as the rigid body rotation does with the transition of γδ resolvase to Gin (Supplementary Movie S3). The modeling of the rotation of a dimer subunit of γδ resolvase as a rigid body about its 2-fold axis (*z*-axis) at the exchange interface results in a near-perfect alignment with the corresponding rotating dimer of Gin (Supplementary Movie S3). This structure-based rotational modeling displays evidence that rotation about the exchange interface is the mechanism of strand exchange in the invertase/resolvase family of serine recombinases.

ACCESSION NUMBERS

3UJ3.

SUPPLEMENTARY DATA

Supplementary Data are available at NAR Online: Supplementary Figures 1–6 and Supplementary Movies 1–4.

ACKNOWLEDGEMENTS

We thank Nigel Grindley for helpful comments while this work was being performed and critical reading of the manuscript. We thank the staff members at APS beam lines 19-ID and 24-ID, Chicago, IL and ALS beam lines 8.2.1/8.2.2, Berkeley, CA, USA.

FUNDING

National Institutes of Health (NIH) [T32 GM007223 to C.J.R. and GM057510 to T.A.S.]; Steitz Center for Structural Biology, Gwangju Institute of Science and Technology, Republic of Korea. Funding for open access charge: NIH [GM057510]

Conflict of interest statement. None declared.

REFERENCES

1. Craig,N.L. (2002) *Mobile DNA II*. ASM Press, Washington, D.C.
2. Guo,F., Gopaul,D. and van Duyne,G. (1997) Structure of Cre recombinase complexed with DNA in a site-specific recombination synapse. *Nature*, **389**, 40–46.
3. Gibb,B., Gupta,K., Ghosh,K., Sharp,R., Chen,J. and Van Duyne,G.D. (2010) Requirements for catalysis in the Cre recombinase active site. *Nucleic Acids Res.*, **38**, 5817–5832.
4. Ghosh,K., Lau,C., Gupta,K. and Van Duyne,G. (2005) Preferential synapsis of loxP sites drives ordered strand exchange in Cre-loxP site-specific recombination. *Nat. Chem. Biol.*, **1**, 275–282.
5. Guo,F., Gopaul,D. and Van Duyne,G. (1999) Asymmetric DNA bending in the Cre-loxP site-specific recombination synapse. *Proc. Natl Acad. Sci. USA*, **96**, 7143–7148.
6. Gopaul,D., Guo,F. and Van Duyne,G. (1998) Structure of the Holliday junction intermediate in Cre-loxP site-specific recombination. *EMBO J.*, **17**, 4175–4187.
7. Grindley,N., Whiteson,K. and Rice,P. (2006) Mechanisms of site-specific recombination. *Annu. Rev. Biochem.*, **75**, 567–605.
8. Li,W., Kamtekar,S., Xiong,Y., Sarkis,G., Grindley,N. and Steitz,T. (2005) Structure of a synaptic gammadelta resolvase tetramer covalently linked to two cleaved DNAs. *Science*, **309**, 1210–1215.
9. Stark,W.M. and Boocock,M.R. (1994) The linkage change of a knotting reaction catalysed by Tn3 resolvase. *J. Mol. Biol.*, **239**, 25–36.
10. Stark,W.M., Sherratt,D.J. and Boocock,M.R. (1989) Site-specific recombination by Tn3 resolvase: topological changes in the forward and reverse reactions. *Cell*, **58**, 779–790.
11. Stark,W.M., Grindley,N.D., Hatfull,G.F. and Boocock,M.R. (1991) Resolvase-catalysed reactions between res sites differing in the central dinucleotide of subsite I. *EMBO J.*, **10**, 3541–3548.
12. Kanaar,R., van de Putte,P. and Cozzarelli,N. (1989) Gin-mediated recombination of catenated and knotted DNA substrates: implications for the mechanism of interaction between cis-acting sites. *Cell*, **58**, 147–159.
13. Dhar,G., Heiss,J. and Johnson,R. (2009) Mechanical constraints on Hin subunit rotation imposed by the Fis/enhancer system and

DNA supercoiling during site-specific recombination. *Mol. Cell*, **34**, 746–759.
14. Li,W. (2004) *Structure of a synaptic gamma-delta resolvase tetramer covalently linked to two cleaved DNAs. Ph.D. Thesis*. Yale University.
15. Yang,W. and Steitz,T. (1995) Crystal structure of the site-specific recombinase gamma delta resolvase complexed with a 34 bp cleavage site. *Cell*, **82**, 193–207.
16. Rice,P. and Steitz,T. (1994) Model for a DNA-mediated synaptic complex suggested by crystal packing of gamma delta resolvase subunits. *EMBO J.*, **13**, 1514–1524.
17. Sanderson,M., Freemont,P., Rice,P., Goldman,A., Hatfull,G., Grindley,N. and Steitz,T. (1990) The crystal structure of the catalytic domain of the site-specific recombination enzyme gamma delta resolvase at 2.7 A resolution. *Cell*, **63**, 1323–1329.
18. Rice,P. and Steitz,T. (1994) Refinement of gamma delta resolvase reveals a strikingly flexible molecule. *Structure*, **2**, 371–384.
19. Kamtekar,S., Ho,R., Cocco,M., Li,W., Wenwieser,S., Boocock,M., Grindley,N. and Steitz,T. (2006) Implications of structures of synaptic tetramers of gamma delta resolvase for the mechanism of recombination. *Proc. Natl Acad. Sci. USA*, **103**, 10642–10647.
20. Keenholtz,R.A., Rowland,S.J., Boocock,M.R., Stark,W.M. and Rice,P.A. (2011) Structural basis for catalytic activation of a serine recombinase. *Structure*, **19**, 799–809.
21. Dhar,G., McLean,M., Heiss,J. and Johnson,R. (2009) The Hin recombinase assembles a tetrameric protein swivel that exchanges DNA strands. *Nucleic Acids Res.*, **37**, 4743–4756.
22. Bai,H., Sun,M., Ghosh,P., Hatfull,G.F., Grindley,N.D. and Marko,J.F. (2011) Single-molecule analysis reveals the molecular bearing mechanism of DNA strand exchange by a serine recombinase. *Proc. Natl Acad. Sci. USA*, **108**, 7419–7424.
23. Altschul,S., Madden,T., Schäffer,A., Zhang,J., Zhang,Z., Miller,W. and Lipman,D. (1997) Gapped BLAST and PSI-BLAST: a new generation of protein database search programs. *Nucleic Acids Res.*, **25**, 3389–3402.
24. Kwoh,D. and Zipser,D. (1981) Identification of the gin protein of bacteriophage mu. *Virology*, **114**, 291–296.
25. Plasterk,R., Brinkman,A. and van de Putte,P. (1983) DNA inversions in the chromosome of Escherichia coli and in bacteriophage Mu: relationship to other site-specific recombination systems. *Proc. Natl Acad. Sci. USA*, **80**, 5355–5358.
26. Plasterk,R., Ilmer,T. and Van de Putte,P. (1983) Site-specific recombination by Gin of bacteriophage Mu: inversions and deletions. *Virology*, **127**, 24–36.
27. Grundy,F. and Howe,M. (1984) Involvement of the invertible G segment in bacteriophage mu tail fiber biosynthesis. *Virology*, **134**, 296–317.
28. Klippel,A., Mertens,G., Patschinsky,T. and Kahmann,R. (1988) The DNA invertase Gin of phage Mu: formation of a covalent complex with DNA via a phosphoserine at amino acid position 9. *EMBO J.*, **7**, 1229–1237.
29. Reed,R. and Grindley,N. (1981) Transposon-mediated site-specific recombination in vitro: DNA cleavage and protein-DNA linkage at the recombination site. *Cell*, **25**, 721–728.
30. Koch,C. and Kahmann,R. (1986) Purification and properties of the Escherichia coli host factor required for inversion of the G segment in bacteriophage Mu. *J. Biol. Chem.*, **261**, 15673–15678.
31. Klippel,A., Cloppenborg,K. and Kahmann,R. (1988) Isolation and characterization of unusual gin mutants. *EMBO J.*, **7**, 3983–3989.
32. Otwinowski,Z. and Minor,W. (1997) *Processing of X-ray Diffraction Data Collected in Oscillation Mode; Methods in Enzymology*. Academic Press, New York.
33. Kabsch,W. (2010) XDS. *Acta Crystallographica Section D*, **66**, 125–132.
34. Wang,J. (2010) Inclusion of weak high-resolution X-ray data for improvement of a group II intron structure. *Acta Crystallogr. D Biol. Crystallogr.*, **66**, 988–1000.
35. Boisvert,D.C., Wang,J., Otwinowski,Z., Horwich,A.L. and Sigler,P.B. (1996) The 2.4 A crystal structure of the bacterial chaperonin GroEL complexed with ATP gamma S. *Nat. Struct. Biol.*, **3**, 170–177.
36. Schwede,T., Kopp,J., Guex,N. and Peitsch,M. (2003) SWISS-MODEL: An automated protein homology-modeling server. *Nucleic Acids Res.*, **31**, 3381–3385.
37. Terwilliger,T. and Berendzen,J. (1999) Automated MAD and MIR structure solution. *Acta Crystallogr. D Biol. Crystallogr.*, **55**, 849–861.
38. Terwilliger,T. (2003) Statistical density modification using local pattern matching. *Acta Crystallogr. D Biol. Crystallogr.*, **59**, 1688–1701.
39. Vagin,A. and Teplyakov,A. (1997) MOLREP: an automated program for molecular replacement. *J. Appl. Cryst.*, **30**, 1022–1025.
40. Murshudov,G., Vagin,A. and Dodson,E. (1997) Refinement of macromolecular structures by the maximum-likelihood method. *Acta Crystallogr. D Biol. Crystallogr.*, **53**, 240–255.
41. Emsley,P. and Cowtan,K. (2004) Coot: Model-building tools for molecular graphics. *Acta Crystallogr. D Biol. Crystallogr.*, **60**, 2126–2132.
42. Carson,M. (1997) Ribbons. *Methods Enzymol.*, **277**, 493–505.
43. Delano,W.L. (2002) DeLano Scientific. *The PyMOL Molecular Graphics System, Version 1.5.0.4 Schördinger, LLC*. San Caros, CA, http://www.pymol.org/ (27 November 2012, date last accessed).
44. Kabsch,W. (1976) A solution for the best rotation to relate two sets of vectors. *Acta Crystallogr. A*, **32**, 922–923.
45. Mouw,K.W., Rowland,S.J., Gajjar,M.M., Boocock,M.R., Stark,W.M. and Rice,P.A. (2008) Architecture of a serine recombinase-DNA regulatory complex. *Mol. Cell*, **30**, 145–155.
46. Mouw,K.W., Steiner,A.M., Ghirlando,R., Li,N.S., Rowland,S.J., Boocock,M.R., Stark,W.M., Piccirilli,J.A. and Rice,P.A. (2010) Sin resolvase catalytic activity and oligomerization state are tightly coupled. *J. Mol. Biol.*, **404**, 16–33.